Performance improvement by alumina coatings on $Y_3Al_5O_{12}$ Ce^{3+} phosphor powder deposited using atomic layer deposition in a fluidized bed reactor

Zhou, Zhi; Zhou, Nan; Lu, Xiangyang; Kate, Melvin Ten; Valdesueiro Gonzalez, D.; van Ommen, J.R.; Hintzen, H. T.

DOI
10.1039/c6ra12983h

Publication date
2016

Document Version
Accepted author manuscript

Published in
RSC Advances

Performance improvement by alumina coatings on $Y_3Al_5O_{12}:Ce^{3+}$ phosphor powder deposited using Atomic Layer Deposition in a fluidized bed reactor

Zhi Zhou[1], Nan Zhou*[1], Xiangyang Lu*[2], Melvin ten Kate[3], David Valdesueiro[4], J. Ruud van Ommen[3], H.T. (Bert) Hintzen[4]

1 Science College of Hunan Agricultural University, Changsha 410128, China
2 College of Bioscience and Biotechnology, Hunan Agricultural University, Changsha 410128, China
3 Department of Chemical Engineering, Delft University of Technology, Van der Maasweg 9, 2629 HZ Delft, The Netherlands
4 Group Luminescent Materials, Section Fundamental Aspects of Materials and Energy, Faculty of Applied Sciences, Delft University of Technology, The Netherlands

Corresponding authors: Dr. Nan Zhou, Email: zhounan@hunau.edu.cn;
Prof. Xiangyang Lu, Email: xiangyangcn@163.com.

Abstract:

To improve the thermal stability, Al_2O_3 has been successfully coated on a $Y_3Al_5O_{12}:Ce^{3+}$ (YAG:Ce) phosphor powder host by using the Atomic Layer Deposition (ALD) approach in a fluidized bed reactor. Transmission Electron Microscopy (TEM) and Energy Dispersive X-ray spectroscopy (EDX) analysis indicate that coating an Al_2O_3 thin layer by ALD is highly feasible. The luminescence properties (such as excitation and emission as well as quantum efficiency and UV-absorption of the coated YAG:Ce phosphor) were systematically analysed, with the further examination of the thermal resistance characteristics. The Al_2O_3 thin layer coating with precisely controlled thickness by ALD can obviously improve theluminescence intensity and greatly enhances the thermal stability of the YAG:Ce phosphor. It is suggested that the alumina coating with tailoring thickness seems not only to act like a barrier to decrease the thermal quenching, but also as a great help to promote the light absorption and transfer.

Key words: Atomic Layer Deposition (ALD), fluidized bed reactor, YAG:Ce, phosphor, powder coating, thermal stability.

1 Introduction

Inorganic luminescent materials, or phosphors, are commonly utilized for many applications such as monitors, fluorescent lamps, plasma displays, X-ray amplifier screens, Light Emitting Diodes (LEDs), and electroluminescent displays due to their cathodo-, photo-, X-ray- or electro-luminescence properties[1-3]. However, the instability of the phosphors against temperature, oxygen, water, acids, etc. remains a problem, which significantly hinders theirprocessing, storage as well as the applications[2].

Coating a phosphor with a protective layer has been proved to be an efficient approach to protect a phosphor from environmental attack[4-12]. Thus, several techniques have been explored to deposit coating layers on phosphor. Including 1) solid-state techniques such as rolling, milling, grinding of mixtures of phosphor powders with the precursor, followed by drying or a heat treatment if necessary; 2) liquid-phase techniques such as sol-gel[4-6], emulsion[7], hetero-coagulation[8], and precipitation[9]; and 3) gas-phase techniques such as Chemical Vapor Deposition (CVD)[10], Pulsed Laser Deposition (PLD)[11], and Atomic Layer Deposition (ALD)[12, 13]. However, most of the conventional coating methods suffer from inhomogeneous and/or ununiformed coating layer deposition, which will has a negative effect on the optical properties[6]. Therefore, a closed thin film coating method is needed in order to protect phosphor particles while maintaining (or even improving) the optical properties.

ALD is well known for depositing thin films on a flat surface, but with the combination of a fluidized bed reactor, it can also be used for coating micro and nano-sized powders[14]. In such a fluidized bed reactor the particles are suspended in an upward gas flow so that good contact between gas and particles is ensured. Besides thin but nevertheless closed coating, another main advantage of ALD is that the thickness of a coated layer can be precisely designed by strictly controlling the number of ALD cycles. Thus, ALD can supply a uniform coating even on high surface area materials allowing a variation of thickness at an atomic resolution, all of which benefits ALD as a suitable method for homogeneous ultrathin layer deposition[15]. Li et al.[16] successfully deposited a 15 nm TiO_2 thin film on Cu_2O-based photocathodes through ALD method after ALD coating of an appropriate 20 nm bufferlayer of Ga_2O_3 on Cu_2O microcrystals. The high thermal resistance of Ga_2O_3 allowed for the double coating at relatively high temperatures, resulting in a better photo-voltage of the whole active cathode. A thin 1.2 nm TiO_2 coating was performed by ALD on cobalt particles to prevent both leaching and sintering during aqueous-phase reactions. The TiO_2/Co/TiO_2 compositeshowed a high catalysis activity foraqueous-phase hydrogenation reactions with excellent stability[17]. All above demonstrate that ALD techniques can produce continuous, pinhole-free oxide films with Angstrom-level-controllable thickness. Especially within a fluidized bed reactor, ALD shows high potential for depositing a protective thin layer coating on a phosphor particle without hurting the optical properties.

Many kinds of the oxides, such as Al_2O_3[18-20], SiO_2[21, 22], TiO_2[23, 24], ZnO[25, 26], and ZrO[27] have been used as coating material in ALD processes. Among them, Al_2O_3 is

considered to be a promising coating agent to enhance the resistance of the coated materials. For example, the capacity fading of $LiMn_2O_4$ spinel as a battery material can be significantly reduced due to Al_2O_3 coating and consistent discharge curves were found even after 50 charging/discharging cycles at an elevated temperature of 55℃ [28]. Ultrathin compact Al_2O_3 layers deposited by ALD were also utilized to improve the ambient stability of quantum dot films[29] and organic-inorganic perovskite solar cells[20]. The results demonstrate that the stability of the solar cell against humidity was greatly enhanced without an obvious reduction in efficiency. Besides, Al_2O_3 demonstrates a unique affinity to a large variety of substrate[14], together with its low deposition temperature, led to the judgments that depositing Al_2O_3 as a coating via ALD in a fluidized bed reactoris a promising way to increase resistance against outside attacks resisted for phosphor materials like $Y_3Al_5O_{12}$: Ce^{3+}.

$Y_3Al_5O_{12}$: Ce^{3+}(the trivalent cerium activated Yttrium Aluminate phosphor with Garnet structure, referred to as YAG:Ce), is a well-known luminescent material which has been broadly applied in the fields of flying spot scanner tubes in the past and white LED (WLED) devices nowadays. However, like most of the luminescence phosphors, YAG:Ce also suffers from the thermal instability, especially when used in practical WLED devices[3]. In this work, YAG:Ce phosphor powderis employed as model material to study the improvement of the thermal stability by Al_2O_3 coating through ALD process performed in a fluidized bed reactor under atmospheric pressure. The impact of ALD cycle numbers on the thickness of the Al_2O_3 layer is investigated, as well as the thermal and optical performance of YAG:Ce phosphor. It will be shown that the ALD method with a fluidized bed reactor using alumina as oxide coating materials could be a feasible way for the ultrathin film coating of YAG:Ce phosphors and apply a protective barrier for improving thermal resistance while maintaining the optical properties.

2 Experimental

2.1 Starting materials

The YAG:Ce phosphor particles were obtained from Steady (Hunan Steady New Materials Company, China), which have a regular spherical morphology with highly concentrated particle size distribution between 6-15 micrometers. Tri-Methyl-Aluminium (TMA, semiconductor grade) was supplied by Akzo-Nobel HPMO in a 400mL VER-400 bubbler. The gas washers were filled with Kaydol oil, supplied by Sonneborn (Haarlem).

2.2 Sample preparation by ALD coating process in a fluidized bed reactor

A schematic illustration of the ALD set-up with a fluidized bed reactor for the alumina coating on YAG:Ce particle is shown in Fig. 1. From left to right, Part A is a nitrogen gas tank supplying a nitrogen flow. Part B is a bubbler filled with liquid TMA, through which nitrogen is bubbled to obtain a nitrogen flow with TMA vapor. Part C is a gas bottle filled with an N_2/O_2 mixture (80%/20%). Part D is the Fluidized Bed Reactor (FBR), the main part of which is a glass column with 26 mm in internal diameter and 500 mm in length. Only less than one third volume of the column can be

filled with certain amount (100-120g) of phosphor particles, in order to guarantee enough space for the particles during fluidizing. The FBR is placed on a vibration table driven by two vibro-motors (Part E), which can produce a low amplitude vibration at a set frequency of 45 Hz to assist fluidization. The coating experiments were carried out at room temperature of about 25°C. And Part F represents the gas washers to neutralize TMA that might be released from the reactor.

Generally, one ALD cycle can be divided into four process steps: (1) TMA exposure, (2) purge with nitrogen gas, (3) oxygen exposure and (4) purge with nitrogen gas again. To begin with the whole ALD set needs to be purged with nitrogen for about 20 min before starting the first ALD cycle. For the first step of TMA exposure, nitrogen was purged through the reactant bubbler (Part B) filled with TMA and making a gas stream for carrying the reactant into the FBR (Part D) with a flow rate of 0.6 L/min (0.02 m/s superficial gas velocity). Subsequently, N_2 was pumped into the reactor to carry away the redundant TMA at the second step. After that, synthetic air was pumped into the reactor to oxidize TMA and form the Al_2O_3 coating. Finally, the extra oxygen was blown away by N_2 and then a new cycle can be started. Duration of each step has been optimized as 3, 10, 3 and 10 minutes, respectively.

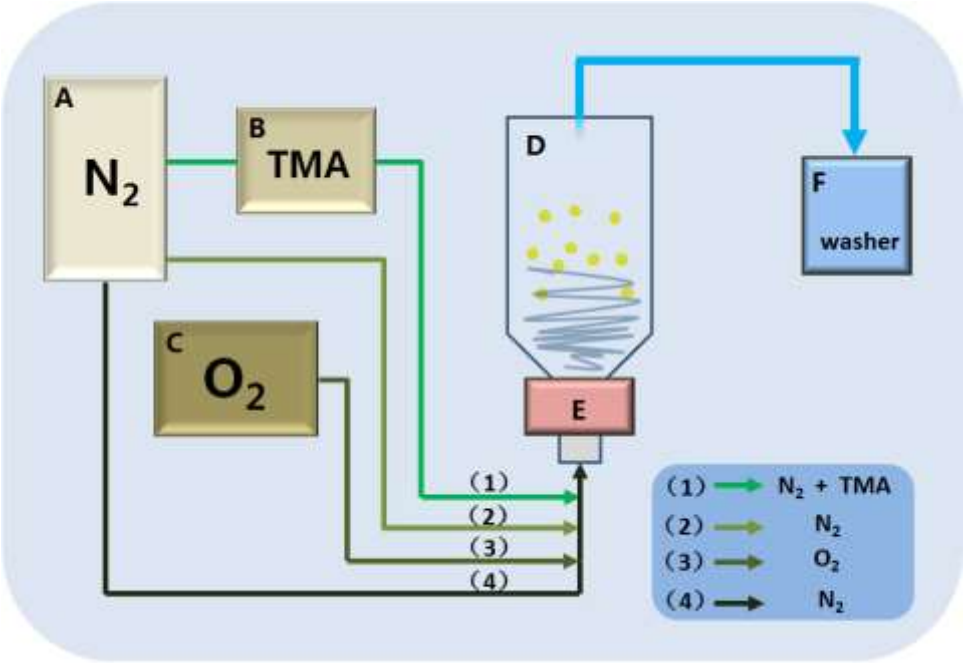

Fig. 1 Schematic illustration of the ALD set-up and process: (A) nitrogen gas tank; (B) and (C) reactant tanks; (D) Fluidized Bed Reactor (FBR); (E) vibro-motors; (F) gas washers.

Effluent gases from the reactor were led through a double set of gas washers (Part F) filled with mineral oil. The gas streams containing TMA was led through separate gas washers to prevent reaction in the washers. Any TMA absorbed in the gas washers was neutralized after the experiment. The effluent from the gas washers was filtered using Pall Kleenpak pharmaceutical grade sterilizing filters to capture elutriated nanoparticles. The pressure at the outlet was atmospheric, meaning that the pressure in the column is slightly above atmospheric pressure. This is uncommon, as

most ALD is carried out at vacuum. More details about the reactor can be found in our previous work[14].

2.3 Characterization

The crystalline phases and compositions of the prepared samples were examined by X-ray diffractometry (XRD) using a Bruker D4 Endeavor apparatus with a graphite- monochromatized Cu Ka radiation at 40 kV and 40 mA. The 2θ ranges of all the data sets are from 10 to 80° using step scan with a step size of 0.02° in 2θ and a counting time of 1s per step.The micro-morphology and elemental mapping of the samples were observed by using a JEOL/EO6500F Scanning Electron Microscope (SEM) combined with Energy Dispersive X-ray spectroscopy (EDX), the voltage of the EDX is 10KV and the spot size is 69 μm. Cross section SEM combined with EDX was carried out on a FEI Nova Nano SEM for the Al_2O_3 coated samples, besides the normal electric-beam for SEM, the equipment has anextra ion-beam for cut and mill the target samples. Moreover, Transmission Electron Microscopy (TEM) analysis was performed with an HRTEM JEOL 2010 high-resolution transmission electron microscope in combination with EDX spectroscopy and a GATAN digital micrograph with a slow-scan CCD camera.

2.4 Optical properties

A Perkin Elmer LS 50B spectrophotometer equipped with a Xe flash lamp as the excitation source was used to conduct diffuse reflectance and photoluminescence (PL) measurements. The reflection spectra were calibrated with the reflection of black felt (reflection 3%) and white barium sulfate ($BaSO_4$, reflection ~100%) in the wavelength region of 230-700 nm. The excitation and emission slits were set at 15 nm. All measurements were performed at room temperature.

The temperature dependent luminescence properties were measured by home-built equipment. The emission spectra were measured in air with the temperature increased from 300K to 600K. The emission spectrum was recorded from 480 nm to 700 nm with an excitation wavelength of 460 nm came from a Xe flash lamp. The sample chamber was heated up with a rate of 10 K/min. The equipment was maintained for extra 5 min before each measurement to hold a constant temperature. The excitation and emission slits were set at 5 nm. Excitation spectra were automatically corrected for the variation in the lamp intensity by a second photomultiplier and a beam-splitter. All the spectra were measured with a scan speed of 100 nm/min.

3 Results and discussion

3.1 Phase composition

To study the impact of the ALD process on the phase composition of the selected phosphor material, uncoated and Al_2O_3 coated Ce-doped YAG phosphor powders were examined by XRD. As shown in Fig. 2, the diffraction peaks of all obtained materials with or without coating are corresponding to $Y_3Al_5O_{12}$ with the garnet structure (YAG) [Joint Committee on Powder Diffraction Standards (JCPDS) card No.

72-1315]. No obvious peak shifts or other impurity phases were detected after the coating process, indicating that the sustainable ALD process has no obvious influence on the phase and structure of the YAG:Ce phosphor. In addition, no diffraction peaks characteristic for crystalline Al_2O_3 were detected, suggesting that the Al_2O_3 thin layer should be amorphous phase since the crystalline phase of Al_2O_3 is expected only above 900°C[30].

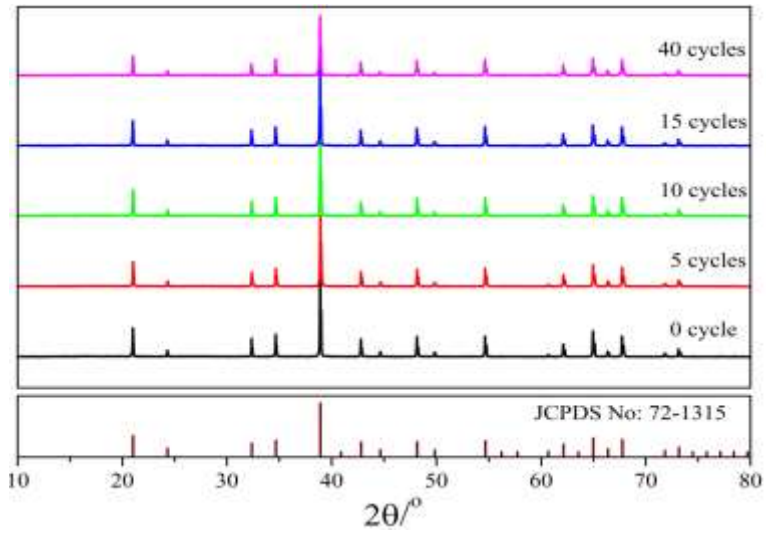

Fig.2 XRD patterns of the uncoated (0 cycle) and coated YAG:Ce phosphor powders after different ALD cycles

3.2 Particle morphology

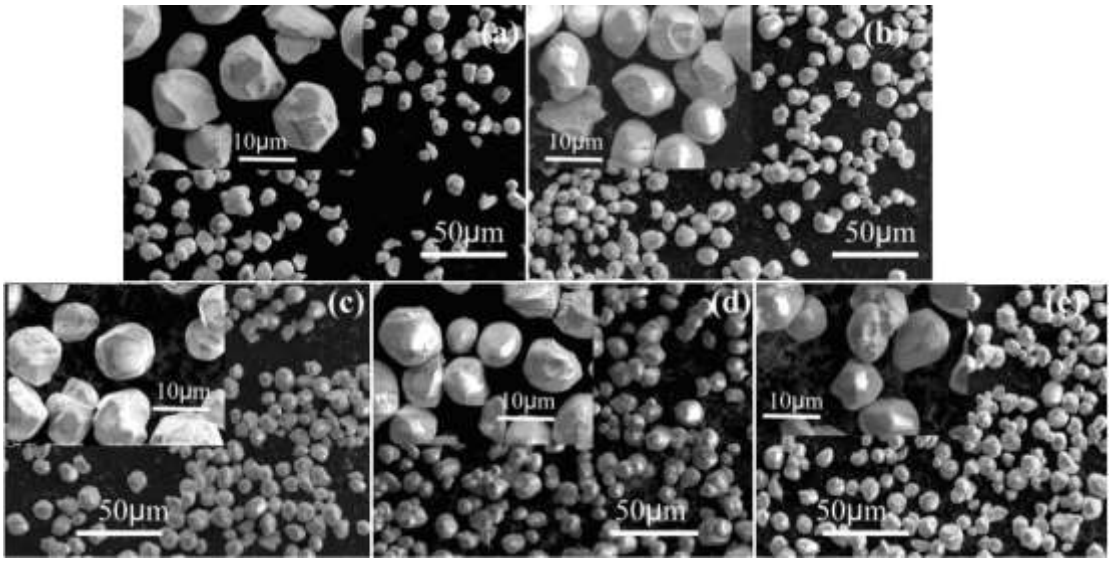

Fig.3 SEM images of (a) the uncoated (0 cycle) and coated samples at different cycles (b) 5 cycles; (c) 10 cycles; (d) 15 cycles; (e) 40 cyclesunder low and high magnification (insets)

SEM analysis was also carried out to investigate the influence of the ALD process and alumina coating on the morphology of YAG:Ce particles. SEM micrographs of the starting YAG:Ce sample [Fig. 3(a)] and Al_2O_3 coated YAG:Ce

particles at various cycles [Fig. 3(b)-3(e)] are shown in Fig. 3. The obtained samples with or without coating show similar micromorphology, all of which consist of uniform and spherical-like particles with a size range of 6-15μm (D_{50} = 11 μm). There is no obvious difference between the coated and uncoated samples, implying that the Al_2O_3 ALD coating process has no influence on the morphology of the YAG:Ce particles, which should attribute to the ultrathin layer of the Al_2O_3 coating that can not be observed by normal SEM.

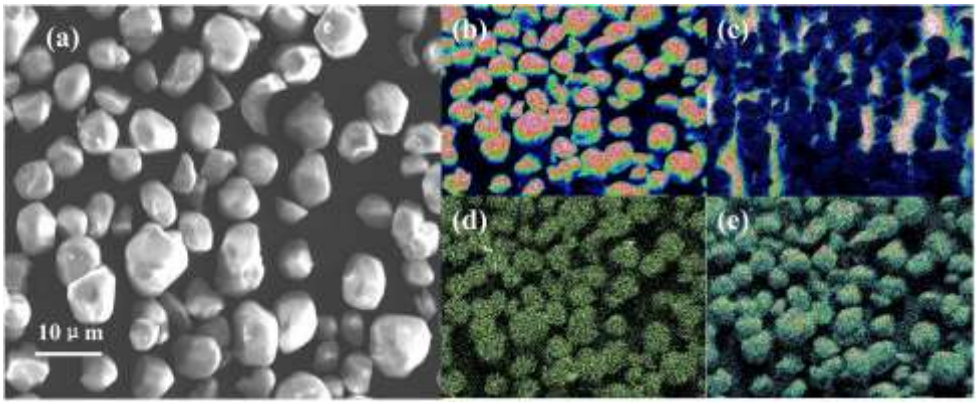

Fig. 4 SEM images of (a) YAG:Ce particle and corresponding elemental mapping of (b) Al, (c) Y, (d) Ce and (e) O.

The elemental distribution of the coated YAG:Ce phosphor was mapped, as illustrated in Fig. 4. Results indicate that the Y, Al, O and Ce elements are uniformly distributed on the same particle, which confirms the uniform and homogeneous coating of alumina via ALD process in fluidized bed. Meanwhile, EDX analysis with SEM shows that the ratio of Al content divided by (Y + Ce) content grows from 1.38 to 1.76 along with the increase of number of ALD cycles, as shown in Table. 1, which should be attributed to the increase of thickness of deposited Al_2O_3 layers with adding more ALD cycles. It needs to be mentioned that the ratio of Al/(Y+Ce) measured by EDX was relatively low compare to the ideal ratio (1.67) calculated for stoichiometric $Y_3Al_5O_{12}$: Ce^{3+}. However, impurities and defects are generally formed during the synthesis of $Y_3Al_5O_{12}$, and they exist within the crystals especially after doping with other cations[31, 32].

Table 1. The dependence of the Al /(Y+Ce) ratio on the number of ALD cycles, as obtained by EDX.

Cycle(s)	0	5	10	15	40
Al/(Y+Ce)	1.38	1.43	1.51	1.60	1.76

Furthermore, cross section SEM by dual beam was performed on the 40 cycles coated sample, as shown in Fig. 5. The signal of Gacomes from the ions beam, which was utilized to section the YAG:Ce particle. According to the EDX examination, the ratio of Al/(Y+Ce) at the surface (spot 2) turns out to be about 3.7, while that in the

bulk (spot 1) is about 1.34, which is in accordance with the Al/(Y+Ce) ratio determined for the uncoated sample (Table. 1). A higher level of Al/(Y+Ce) ratio at the surface than in the inner part of the particle, demonstrates that Al_2O_3 had been depositedon the surface of the phosphor particle and Al_2O_3 thin layer coating with ALD is highly feasible.

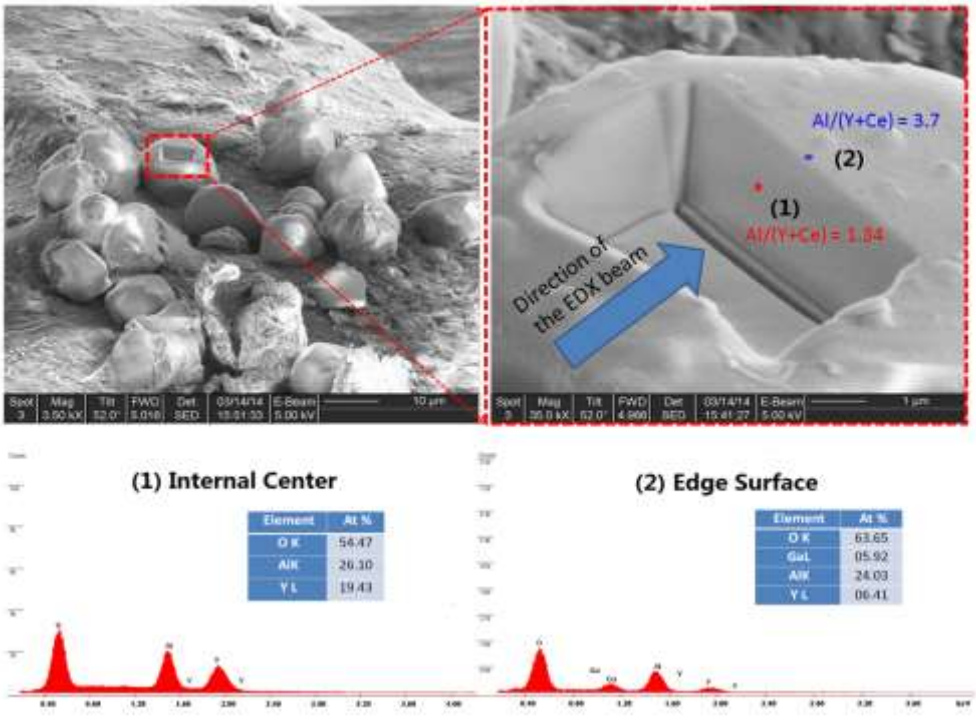

Fig.5 SEM cross section combined with EDX analysis of 40 cycles ALD coated YAG:Ce particle

To further study the thickness of the ALD coating, TEM images of the coated samples were made. Unfortunately, the alumina layers covering the surface of the YAG:Ce particles were too thin to be observed for 5 and 10 cycles coated samples. But after 15 cycles of ALD coating, a 2 nm coating layer was detected and a clearer layer with 5 nm thickness was found for the sample coated with Al_2O_3 for 40 cycles by ALD process, TEM images are shown in Fig. 6. Besides, the alumina coating layers of both samples processed after 15 and 40 cycles were uniform, tight, and homogeneous, indicating that the ALD process performed in a fluidized bed is a promising approach for covering protective materials on phosphor particles. The thickness of the coating layer on the particles after 15 and 40 cycles is about 2 nm and 5 nm, respectively, from which the thickness of a single layer coating within one cycle can be estimated to be about 0.13 nm.

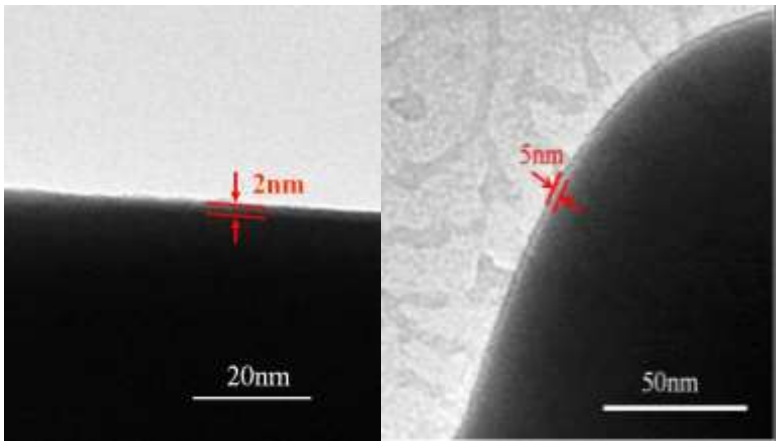

Fig. 6 TEM images of YAG:Ce particle coated with Al_2O_3 by ALD: (a) 15 cycles and (b) 40 cycles.

3.3 Luminescence properties

It has been confirmed that Al_2O_3 is an appropriate material for thermal protection via ALD process[33]; however, it can also become an impeder for transfer of light, electrons, heat, humidity and so on[34]. Thus, the luminescence properties of coated and uncoated YAG:Ce phosphor powders were carefully investigated in order to optimize the ALD cycle numbers and alumina coating thickness. Fig. 7 displays the luminescence spectra of uncoated YAG:Ce powder and Al_2O_3 coated YAG:Ce powders with different ALD cycle numbers. It can be seen that all samples, with or without coating, exhibit similar profiles of both excitation and emission bands with the same peak positions located atabout 535 nm, indicating that the basic optical behavior of the phosphor has not been changed by the coating layer of alumina. The excitation spectra of all samples obtained upon monitoring 535 nm emission express two bands centered at around 450 nm and 350 nm respectively, which are corresponding to the transitions between the Ce^{3+} ground state ($^2F_{5/2}$) and the 5d levels splitted by the crystal field with D_2 symmetry, which is in agreement with the report in the literature[35]. Upon 460 nm excitation, all the samples show a broad band emission with the maximum peaks located at about 535 nm, which is assigned to the transition of the lowest 5d state to the 4f ground state ($^2F_{5/2}$) of Ce^{3+} ions.

Some experimental results from Zhang et al.[36] confirm that the optical absorptionbehavior of phosphor composite materialscan belargely dependent on the amount of Al_2O_3 compound. However, results achieved above indicate that the Al_2O_3 coating has no obvious affection on the luminescence properties of the sample. The reason might be that the alumina-coating layer is too thin to affect the light diffusion.

Nevertheless, the intensity of both excitation and emission bands show significant difference when comparing the uncoated and coated samples. The excitation and emission intensity continuously increase with increasing ALD cycle numbers, except for 40 cycles. After 40 cycles coating, the intensity dropped quite strongly and a value even lower than the uncoated phosphor was obtained. It can be concluded that alumina coating layer with controlled thickness of about 2 nm deposited via ALD process can benefit the luminescence properties, but too thick a coating will lower the excitation absorption as well as the emission radiation. The

enhancement of emission intensity can be attributed to an increased absorption radiation, a larger quantum efficiency of absorbed radiation converted into emitted radiation and an improved light outcoupling of emitted radiation. But when the thickness of the covering went to 5 nm, the incident illumination and the emitted light were largely obstructed by the over protective covering, thus the intensity of both excitation and emission decreased rapidly.

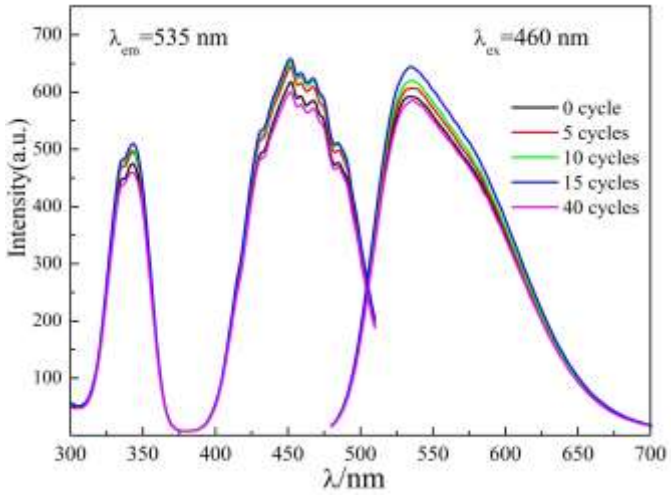

Fig.7 Excitation and emission spectra of the uncoated and ALD coated YAG:Ce phosphor powder (a) 0 cycle; (b) 5 cycles; (c) 10 cycles; (d) 15 cycles ; (e) 40 cycles.

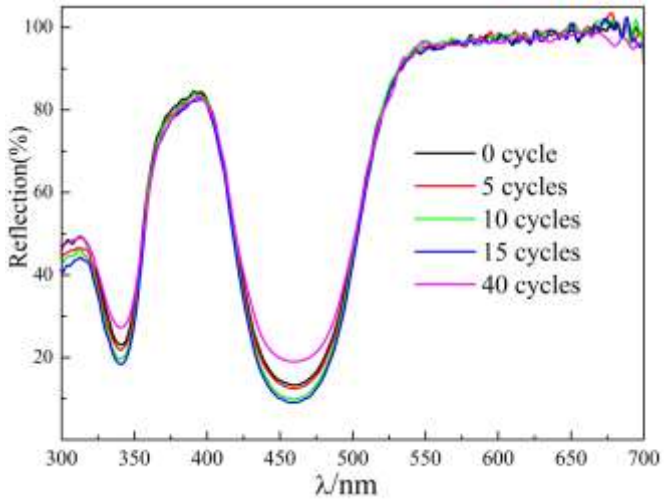

Fig.8 Diffuse reflectance spectra of the uncoated (0 cycles) and Al_2O_3 coated YAG:Ce samples for different ALD cycles (5-40 cycles)

A further illustration about the increased absorption strength is provided by the diffuse reflectance spectra of coated and uncoated samples as shown in Fig. 8. In comparison with the uncoated YAG:Ce samples, the Al_2O_3 coated ones with different number of cycles exhibit similar absorption profiles and band widths, confirming that the Al_2O_3 coating material has no significant effect on the absorption characteristics of

YAG:Ce phosphor powder. As compared to the uncoated phosphor, the reflection (around 340 and 455 nm) decreased (i.e. adsorption around 340 and 455 nm increased) for higher number of ALD cycles, except for the 40 cycles sample (Table 2). All of the above results are in agreement with the conclusion made from Fig. 7, further confirming that the covering thickness of the alumina coating should be optimized since a high amount of Al_2O_3 can hamper the light absorption as well as the light emission (Table 2).

The relative quantum efficiency is estimated by comparing the emission intensity (EI) of the coated sample with that of the uncoated YAG:Ce phosphor powder from the equation below:

$$QE\,(coated) = \left[\frac{EI\,(coated)}{EI\,(uncoated)}\right] * \left[\frac{A\,(uncoated)}{A\,(coated)}\right] * QE\,(uncoated)$$

Here, "QE" refers to the relative quantum efficiency; "EI" refers to the integrated area under the emission spectrum, which was obtained from the emission spectra in Fig. 7; "A" refers to the absorption intensity at excitation wavelength of 460 nm, which was calculated from the diffuse reflection spectra (A=1 - diffuse reflectionfor semi-infinite thick samples). The QE of the uncoated phosphor was taken 1.00. The calculated relative QE for the uncoated and coated samples are listed in Table. 2. The emission intensity of the phosphors increased with the adding of cycle numbers, and so does the relative quantum efficiency, with an exception of the 40 cycles coating sample. The higher relative quantum efficiency is attributed to surface passivation (resulting in less non-radiative transitions at defects) and easier extraction of the emitted light. In summary, the results indicate that the coated YAG:Ce samples processed with10-15 cycles have better conversion abilities than the uncoated material.

Table 2. The absorption of 460 nm (excitation radiation) and the relative quantum efficiency of Al_2O_3 coated versus uncoated YAG: Ce phosphor powders.

Number of coating cycles	Emission (arb. Units)	Absorption at 460 nm	Relative Quantum Efficiency
0 cycle	61639	0.93	1.00
5 cycles	63070	0.94	1.01
10 cycles	64222	0.94	1.03
15 cycles	66525	0.95	1.06
40 cycles	52938	0.93	0.96

3.4 Thermal stability

Fig. 9 displays the temperature-dependent emission spectra of the uncoated and coated YAG:Ce phosphor powders prepared by ALD method, combined with the summary of the dependence of the emission intensity in sample temperature (Fig. 9(d)). When compared with the uncoated YAG:Ce phosphor, the peak emission

wavelength of all the coated samples shows a red shift for higher sample temperature, which can be explained by increased re-absorption due to more efficient energy transfer at high temperature. When excited by 460 nm radiation, the integrated emission intensities of all the samples continuously decreased with increasing sample temperature from 300K to 600K, showing a typical thermal quenching behavior, which is a normal phenomenon for all kinds of phosphors[3]. In comparison with the uncoated sample, a remarkable development in temperature-dependent characteristic of Ce^{3+} emission of coated phosphors can be observed, demonstrating that the thermal stability of YAG:Ce phosphor can be significantly improved by coating protective alumina layers via ALD method.

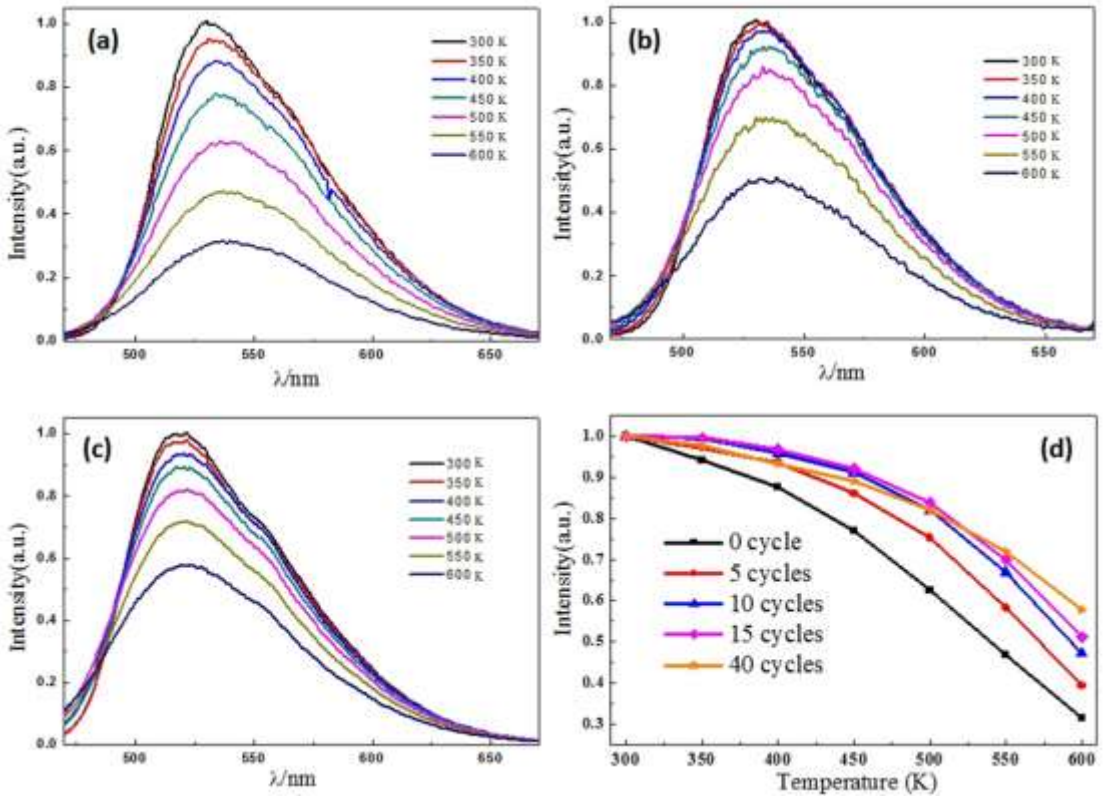

Fig.9 Temperature-dependent PL spectra for samples with various coating cycles: (a) uncoated, (b) 15 cycles, (c) 40 cycles, and (d) summarization of the PL intensity ofall samples, under excitation wavelengths of 460 nm.

Fig. 9(d) summarizes the emission intensity at different temperatures of all samples according to the temperature-dependent emission spectra. The intensity was normalized to that exhibited at room temperature for each sample. At the starting temperature of 300K, all five samples are normalized as the same emission intensity of about 100% for comparison. However, already after 50 degrees temperature increment, remarkable changes have been observed for the alumina coated YAG:Ce phosphor powders. More than 5% decrease was found for the uncoated phosphor, while the intensity of the 5 cycles sample dropped only about 2% and the intensity of samples with 10 and 15 cycles coating remainedmore or less constant. The thermal

stability of the coated phosphor has been remarkably improved even for only 5 ALD coating cycles, and for higher ALD cycle numbers, better thermal stability can be achieved. Especially at elevated temperature of 550K and 600K, the emission intensity of the uncoated phosphor dropped rapidly to 47% and 32%, while that of the 40 cycles coated sample remained at a high value of 70% and 57%, respectively. The enhancement of thermal stability should be attributed to the effect of the thermal barrier coating of alumina formed by ALD process, which can keep the inner phosphor particles from directly exposure to the hot environment and protect Ce^{3+} against oxidization to Ce^{4+}.

A phenomenon needs to be mentioned is that a lower relative emission intensity was exhibited by sample with 40 cycles coating than that of samples with 10 and 15 cycles coating during the temperature range of 300K to 500K, indicating that high thickness alumina layer coatings might impede the luminescence properties of the phosphor below 550 K. It has been reported that Al_2O_3 sometimes works like an insulator that can barrier the transfer of light, electrons or heat[34]. This conclusion is in accordance with the results of the luminescence property analysis discussed above.

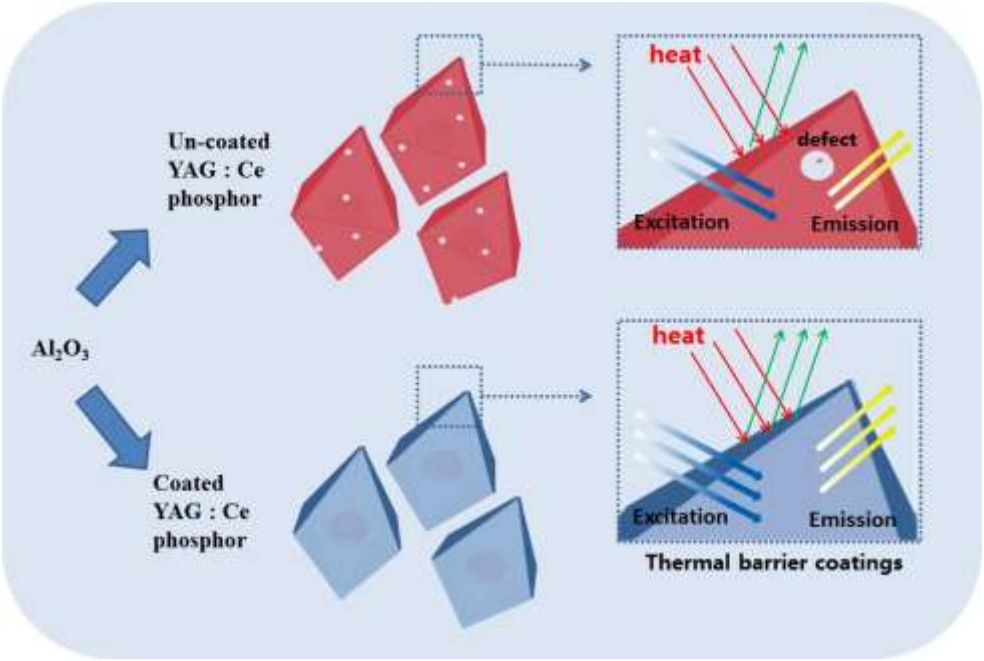

Fig.10 Schematic diagram of enhancing of luminescence intensity coating Al_2O_3 layer by ALD process in YAG:Ce host.

Fig. 10 schematically illustrates the mechanism of the enhancing emission intensity and thermal stability from the protective alumina layer for YAG:Ce phosphor. Firstly, coating the YAG:Ce phosphor powders with a thin Al_2O_3 layer with an appropriate thickness can increase the quantum efficiency due to reduced number of surface defects,enhance the light absorption and form a thermal barrier coating. Secondly, Al_2O_3 is kind of wide band gap oxide material, which could confine the inside excitation of the phosphor and suppress the ion-ion energy transfer (short range Forster transfer), ultimately decrease the non-radiative recombination. Finally, the

lack of Ce ion in the outer coating shell would effectively suppress the energy transfer from the inner part of the particle to the outside surface.Combined the above three, the quantum efficiency, emission intensity as well as thermal stability of the phosphor can be remarkably improved.

4 Conclusions

The yellow-emitting YAG:Ce LED phosphor powders have been successfully coated with a thin Al_2O_3 layer via the approach of fluidized bed reactor ALD. With the controllable deposition in the fluidized bed ALD reactor, designable thickness of the alumina-coating layer can be obtained. With the appropriate Al_2O_3 coating layer thickness, an improvement of luminescence properties and thermal stability of the phosphor can be achieved without any change in bulk behavior. The uniform and stable Al_2O_3 coating can reduce the number of surface defects of the phosphor particles and might enhance the quantum efficiency, consequently improving the optical performance. The thermal stability was improved gradually with the increase of the coating layer thickness, since the coated layer can act as a barrier to decrease the thermal quenching, resulting in high thermal resistance of the YAG:Ce material. For all the samples examined, the one with 15 cycles coating exhibited the best characteristics, from which can be concluded that the amount of the alumina coating needs to be precisely controlled.

Acknowledgement

The authors would like to thank the China Scholarship Council (No 201206370063), the Education Department of Hunan Province (No 14C0577), Hunan NaturalScience Foundation (2016JJ3065), and Hunan Agricultural University (No 13YJ02, No 14YJ05) for financial support.

Reference:

1. T. Jüstel, H. Nikol and C. Ronda, *Angewandte Chemie International Edition*, 1998, **37**, 3084-3103.
2. Y. Li, M. Gecevicius and J. Qiu, *Chemical Society Reviews*, 2016, **45**, 2090-2136.
3. G. Li, Y. Tian, Y. Zhao and J. Lin, *Chemical Society Reviews*, 2015, **44**, 8688-8713.
4. H. Kim, C. Yun, S. W. Jeon, J. K. Lee and J. P. Kim, *Optical Materials*, 2016, **53**, 48-53.
5. J. Zhang, Y. Fan, Z. Chen, S. Yan, J. Wang, P. Zhao, B. Hao and M. Gai, *Journal of Rare Earths*, 2015, **33**, 922-926.
6. J. P. Kim and S. B. Song, *Applied Surface Science*, 2011, **257**, 2159-2163.
7. H. Yang, X. Wang, G. Duan, Y. Cui, L. Shen, Y. Xie and H. Sangdo, *Materials Letters*, 2004, **58**, 2374-2376.
8. H. S. Park, G. Dodbiba, L. F. Cao and T. Fujita, *Journal of Physics: Condensed Matter*, 2008, **20**, 204105.
9. H. Zhu, H. Yang, W. Fu, P. Zhu, M. Li, Y. Li, Y. Sui, S. Liu and G. Zou, *Materials Letters*, 2008, **62**, 784-786.
10. K. L. Choy, *Progress in Materials Science*, 2003, **48**, 57-170.

11. J. Chao, L. Fei, L. Hua, H. Shao-liu, L. Bo and W. You-qing, *Applied Surface Science*, 2005, **246**, 207-213.
12. O. J. Kilbury, K. S. Barrett, X. Fu, J. Yin, D. S. Dinair, C. J. Gump, A. W. Weimer and D. M. King, *Powder Technology*, 2012, **221**, 26-35.
13. N. Avci, J. Musschoot, P. F. Smet, K. Korthout, A. Avci, C. Detavernier and D. Poelman, *Journal of The Electrochemical Society*, 2009, **156**, J333-J337.
14. R. Beetstra, U. Lafont, J. Nijenhuis, E. M. Kelder and J. R. van Ommen, *Chemical Vapor Deposition*, 2009, **15**, 227-233.
15. M. Ritala, K. Kukli, A. Rahtu, P. I. Räisänen, M. Leskelä, T. Sajavaara and J. Keinonen, *Science*, 2000, **288**, 319-321.
16. Z. Wang, H. Guo, F. Shen, G. Yang, Y. Zhang, Y. Zeng, L. Wang, H. Xiao and S. Deng, *Chemosphere*, 2015, **119**, 646-653.
17. J. Lee, D. H. K. Jackson, T. Li, R. E. Winans, J. A. Dumesic, T. F. Kuech and G. W. Huber, *Energy & Environmental Science*, 2014, **7**, 1657-1660.
18. M. Zeng, X. Peng, J. Liao, G. Wang, Y. Li, J. Li, Y. Qin, J. Wilson, a. song and S. Lin, *Physical Chemistry Chemical Physics*, 2016, DOI: 10.1039/C6CP01299J.
19. L. H. Kim, Y. J. Jeong, T. K. An, S. Park, J. H. Jang, S. Nam, J. Jang, S. H. Kim and C. E. Park, *Physical Chemistry Chemical Physics*, 2016, **18**, 1042-1049.
20. X. Dong, X. Fang, M. Lv, B. Lin, S. Zhang, J. Ding and N. Yuan, *Journal of Materials Chemistry A*, 2015, **3**, 5360-5367.
21. J. D. Ferguson, A. W. Weimer and S. M. George, *Chemistry of Materials*, 2000, **12**, 3472-3480.
22. J. Lu, Y. H. Wang, J. B. Zang and Y. N. Li, *Applied Surface Science*, 2007, **253**, 3485-3488.
23. K. Nevalainen, R. Suihkonen, P. Eteläaho, J. Vuorinen, P. Järvelä, N. Isomäki, C. Hintze and M. Leskelä, *Journal of Vacuum Science & Technology A*, 2009, **27**, 929-936.
24. P. A. Williams, C. P. Ireland, P. J. King, P. A. Chater, P. Boldrin, R. G. Palgrave, J. B. Claridge, J. R. Darwent, P. R. Chalker and M. J. Rosseinsky, *Journal of Materials Chemistry*, 2012, **22**, 20203-20209.
25. D. M. King, J. Li, X. Liang, S. I. Johnson, M. M. Channel and A. W. Weimer, *Crystal Growth & Design*, 2009, **9**, 2828-2834.
26. D. M. King, X. Liang, P. Li and A. W. Weimer, *Thin Solid Films*, 2008, **516**, 8517-8523.
27. J. Zhao and Y. Wang, *Nano Energy*, 2013, **2**, 882-889.
28. L. Xiong, Y. Xu, T. Tao, X. Du and J. Li, *Journal of Materials Chemistry*, 2011, **21**, 4937-4944.
29. D. Valdesueiro, M. K. Prabhu, C. Guerra-Nunez, C. S. S. Sandeep, S. Kinge, L. D. A. Siebbeles, L. C. P. M. de Smet, G. M. H. Meesters, M. T. Kreutzer, A. J. Houtepen and J. R. van Ommen, *The Journal of Physical Chemistry C*, 2016, **120**, 4266-4275.
30. H. J. Kim, M. W. Kim, H. s. Kim, H. S. Kim, S. H. Kim, S. W. Lee, B. H. Choi, B. K. Jeong and H. h. Lee, *Molecular Crystals and Liquid Crystals*, 2006, **459**, 239/[519]-245/[525].
31. H. K. Yang, H. M. Noh and J. H. Jeong, *Solid State Sciences*, 2014, **27**, 43-46.
32. M. Kučera, K. Nitsch, M. Nikl and M. Hanuš, *Radiation Measurements*, 2010, **45**, 449-452.
33. V. Edlmayr, M. Moser, C. Walter and C. Mitterer, *Surface and Coatings Technology*, 2010, **204**, 1576-1581.
34. A. Kafizas and I. P. Parkin, *Chemical Society Reviews*, 2012, **41**, 738-781.
35. Z. Zhi, L. Suqin, W. Fengchao and L. Younian, *Journal of Physics D: Applied Physics*, 2012, **45**, 195105.

503 36. C. Zhang and J. Lin, *Chemical Society Reviews*, 2012, **41**, 7938-7961.